Influence of the Diffuse Layer Overcharging or Undercharging on the Stability of Charged Interfaces: A Restricted Grand Canonical Monte Carlo Study

Alfred Delville*

CRMD, CNRS, 1B rue de la Férollerie, 45071 Orléans Cedex 02, France

Received: September 8, 2004; In Final Form: November 15, 2004

We have applied a restricted grand canonical Monte Carlo procedure to describe, in the framework of the primitive model, the counterion exchange mechanism between diffuse layers of counterions surrounding segregated charged lamellae. The net charge transfer between the dense and dilute domains is shown to vary as a function of the valence of the neutralizing counterions: undercharging of the dense interlayer is detected in the presence of monovalent counterions and overcharging with divalent counterions. Furthermore, no net reduction of the swelling pressure is detected for monovalent counterions, while a large enhancement of the net interlamellar attraction is found for charged lamellae neutralized by divalent counterions.

(I) Introduction

The electrostatic contribution to the stability of charged interfaces is a central factor, monitoring the mechanical behavior of a large class of materials (such as clay swelling or cement setting)[1−3] implied in many industrial applications (civil engineering, waste management, water treatment, etc).[1−3] The long range electrostatic repulsion between charged colloids [latex, mineral oxides (such as silica or clays), and biopolymers (such as DNA or polysaccharides)] is generally described on the basis of the Deryaguin−Landau−Verwey−Overbeek (DLVO) theory[4−6] which quantifies, in the framework of the cell mode,[7] the balance between the counterions/surface contact repulsion and electrostatic attraction by the local ionic density at half separation between the charged surface.[1] This property is the direct consequence of the electroneutrality of the Wigner cell centered on one isolated charged colloid and its surrounding counterions.[8] In that context, the swelling pressure results from a difference between the counterion activity inside two well defined macroscopic phases: the reservoir of bulk water and the dense colloidal dispersion. This approach was shown to describe successfully the mechanical behavior of a large class of charged materials neutralized by monovalent counterions,[9−12] since the neglected interionic correlation forces then remain negligible. Under stronger electrostatic coupling (i.e., for charged interfaces neutralized by di- or polyvalent counterions), the interionic correlation force becomes important[13−16] and overcomes the repulsion resulting from the overlap of the diffuse layers surrounding each charged colloid. Numerical simulations were already performed to carefully quantify the net mechanical behavior resulting from the two supplementary contributions induced by these interionic correlations (i.e., electrostatic attraction and excluded volume repulsion),[17−19] generally leading to a net interparticle attraction at weak separation (one or two ionic diameters).

However, this macroscopic separation between two well identified phases is sometimes difficult to figure out for some experimental systems such as flocs or a dense set of particles immersed in a solution or experimental setups used for atomic force microscopy (AFM)[20] or surface force apparatus (SFA)[1]. For such open systems, one can easily identify ionic diffusion as a simple mechanism responsible for the equilibration of the counterion activity within the whole system, leading, at equilibrium, to the cancellation of the net repulsion resulting from the overlap of the diffuse layer. Of course, each subsystem, that is, the dense ensemble of charged particles (flocs) or the two approaching crossed cylinders (SFA), on one hand, and the remote solution, on the other hand, bears a net electric charge but *the whole system remains electrically neutral*. The purpose of this study is to determine the influence of such an ionic exchange mechanism on the electrostatic stability of charged interfaces neutralized by mono- and divalent counterions. Does this mechanism lead to some overcharging or undercharging of the diffuse layer of counterions confined between the charged interfaces? Removing the constraint concerning the local electroneutrality of each subsystem may lead to a net reduction of the free energy of these charged interfaces by comparison with the predictions of the classical DLVO theory. In addition, one may expect, in the presence of divalent counterions, an enhancement of interionic correlations[21,22] due to larger fluctuations of the local ionic densities.

To settle these questions, we have performed Monte Carlo simulations of the distribution of mono- and divalent counterions between two infinite charged lamellae immersed within a large simulation cell. The stability of the charged interface is determined by two independent procedures either by a calculation of the net force acting on the lamellae or by a direct derivation of the entropy of the interface including the first-order contribution from the interionic correlations.[23] A first set of simulations is performed by using the classical canonical Monte Carlo procedure[26] and maintaining the electrical neutrality of each subsystem (i.e., the confined diffuse layer and the remote surfaces). The equilibration between the counterion activities of the two subsystems is then performed by a restricted grand canonical Monte Carlo procedure which simultaneously removes one counterion from a randomly selected subsystem and adds it to the remaining subsystem, thus preserving the electrical neutrality of the whole system.

(II) Methods

(A) Electrostatic Energy. The Monte Carlo simulations are performed for two charged lamellae (thickness 10 Å) centered on the origin and immersed in a large simulation cell (length 830 Å, width 800 Å). Two surface charge densities were

* To whom correspondence should be addressed. E-mail: delville@cnrs-orleans.fr.

10.1021/jp045949c CCC: $30.25
Published on Web 01/07/2005

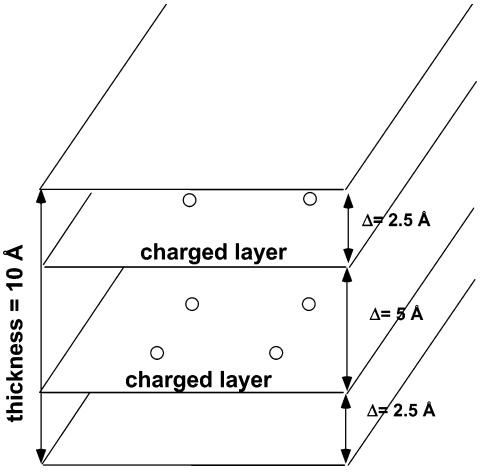

Figure 1. Schematic view of the distribution of the electric charges within a lamella.

considered, with 6272 or 12 800 monovalent electric charges per lamella. These charges are distributed in two squared networks, each located at 2.5 Å from the basal surfaces of the lamellae (see Figure 1). The average surface densities of the lamellae are respectively 4.9×10^{-3} and 1.0×10^{-2} e/Å^2, that is, the order of magnitude of the surface charge density of various metallic oxides,[25] including clay minerals[26] or cement[20] particles. In the framework of the primitive model,[27] the interactions between the solvated ions are described by

$$u(r_{ij}) = \frac{q_i q_j}{4\pi\epsilon_0\epsilon_r r_{ij}}, \quad \text{if } r_{ij} \geq a_i + a_j \tag{1a}$$

$$u(r_{ij}) = \infty, \quad \text{elsewhere} \tag{1b}$$

where a_i is the ionic radius. Our simulations were performed with radii equal to 2.125 and 2.5 Å to mimic hydrated sodium and calcium counterions,[28] respectively.

Ewald summation[29] is used in addition to the minimum image convention[24] in order to calculate the electrostatic energy of the interfaces, by summing the repulsive (lamella/lamella and ion/ion) and attractive (ion/lamella) electrostatic contributions:

$$E_{\text{elect}} = E_{\text{dir}} + E_{\text{rec}} + E_{\text{self}} \tag{2a}$$

$$E_{\text{dir}} = \frac{1}{8\pi\epsilon_0\epsilon_r}\sum_{i=1}^{N_i} q_i \sum_{j=1,i\neq j}^{N_j} \frac{q_j \operatorname{erfc}(\alpha r_{ij})}{r_{ij}} \tag{2b}$$

$$E_{\text{rec}} = \frac{1}{2V\epsilon_0\epsilon_r}\sum_{\vec{K},|K|\neq 0} \frac{\exp(-|\vec{K}|^2/4\alpha^2)}{|\vec{K}|^2} \left[\left\{\sum_i q_i \cos(\vec{K}\times\vec{r}_i)\right\}^2 + \{\sum_j q_j \sin(\vec{K}\times\vec{r}_j)\}^2\right] \tag{2c}$$

$$E_{\text{self}} = \frac{-\alpha}{4\pi^{3/2}\epsilon_0\epsilon_r}\sum_i q_i^2 - \frac{1}{8\pi\epsilon_0\epsilon_r}\sum_{\alpha=1}^{n_\alpha}\sum_{i=1}^{n_\alpha} q_i \sum_{j=1,j\neq i}^{n_\alpha} \frac{q_j \operatorname{erf}(\alpha r_{ij,\alpha})}{r_{ij,\alpha}} \tag{2d}$$

where the second term of eq 2d is evaluated for the set of electric charges located on the same lamella. The simulations were performed with $\alpha = 7.5 \times 10^{-3}$ Å^{-1} and with 2196 replicas in the reciprocal space summation, leading to an estimate of the electrostatic energy with an accuracy better than 0.003.[30] The temperature was taken to be 298 K for salt-free suspensions.

(B) Net Interlamellar Pressure. The interlamellar pressure is also derived from the results of the Monte Carlo simulations

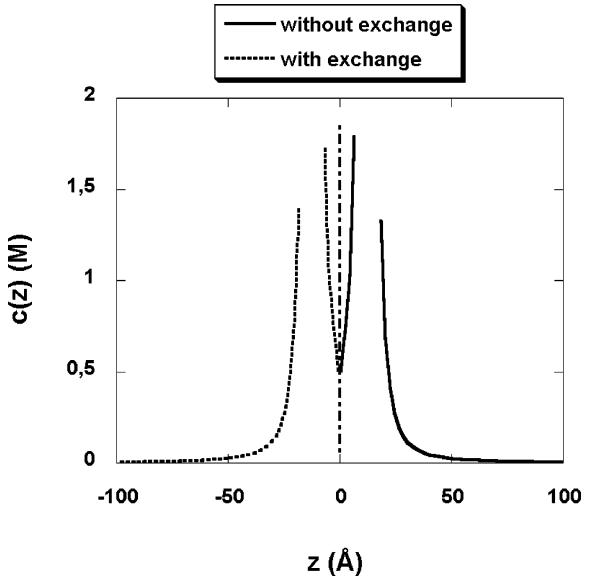

Figure 2. Concentration profiles of the neutralizing monovalent counterions condensed between two lamellae with a period of 25 Å without (continuous curve) or with (discontinuous curve) ionic exchange between the inner and outer domains.

by dividing the net force acting on the lamellae by their cross section. In the framework of the primitive model, the force acting on the lamellae results from the electrostatic (lamella/lamella repulsion and ion/lamella attraction) and the contact ion/lamella contributions. Ewald summation is also used to derive the electrostatic contribution to the force:[29]

$$\vec{F}_{\text{el}}^{\text{dir}} = \sum_{i\in p} q_i \sum_{j\notin p} q_j \left[\frac{2\alpha r_{ij}\exp(-\alpha^2 r_{ij}^2) + \sqrt{\pi}\operatorname{erfc}(\alpha r_{ij})}{4\pi^{3/2}\epsilon_0\epsilon_r}\right]\frac{\vec{r}_{ij}}{r_{ij}^3} \tag{3a}$$

$$\vec{F}_{\text{el}}^{\text{rec}} = \frac{-1}{\epsilon_0\epsilon_r V}\sum_{i\in p} q_i \sum_{\vec{K},|K|\neq 0} \frac{\vec{K}\exp(-|\vec{K}|^2/4\alpha^2)}{|\vec{K}|^2}\sum_j q_j \sin(\vec{K}\times\vec{r}_{ij}) \tag{3b}$$

The contact repulsion is evaluated from the ionic concentration profiles (see Figure 2) describing the distribution of the counterions between the lamellae and outside the interlamellar domains:

$$P_{\text{cont}} = \frac{kT}{S}\int_{\text{surf}} (c_i^{\text{intra}}(0) - c_i^{\text{extra}}(0))\, \text{ds} \tag{4}$$

where S is the cross section of the lamellae and $c^{\text{intra}}(0)$ and $c^{\text{extra}}(0)$ are the ionic density in contact with the lamellae in the intralamellar and outer lamellar domains, respectively. Since the maximum interlamellar separation is 100 Å (see Figure 3), the contact densities in the outer lamellar domain is not sensitive to the overlap between their diffuse layers of counterions. Because of the ionic condensation phenomenon, the local density of the counterions varies steeply near the charged lamellae (see Figure 2). The contact densities used in eq 4 are thus extrapolated by fitting the ionic densities on a quadratic law by using a set of five separations ranging between 0.1 and 0.5 Å. Since these separations are smaller than the ionic radius, this procedure was shown to lead to reliable results.[23]

(C) Direct Derivation of the Entropy. As shown many years ago,[31−32] interionic correlations may be explicitly introduced in the derivation of the interfacial entropy by using the distribu-

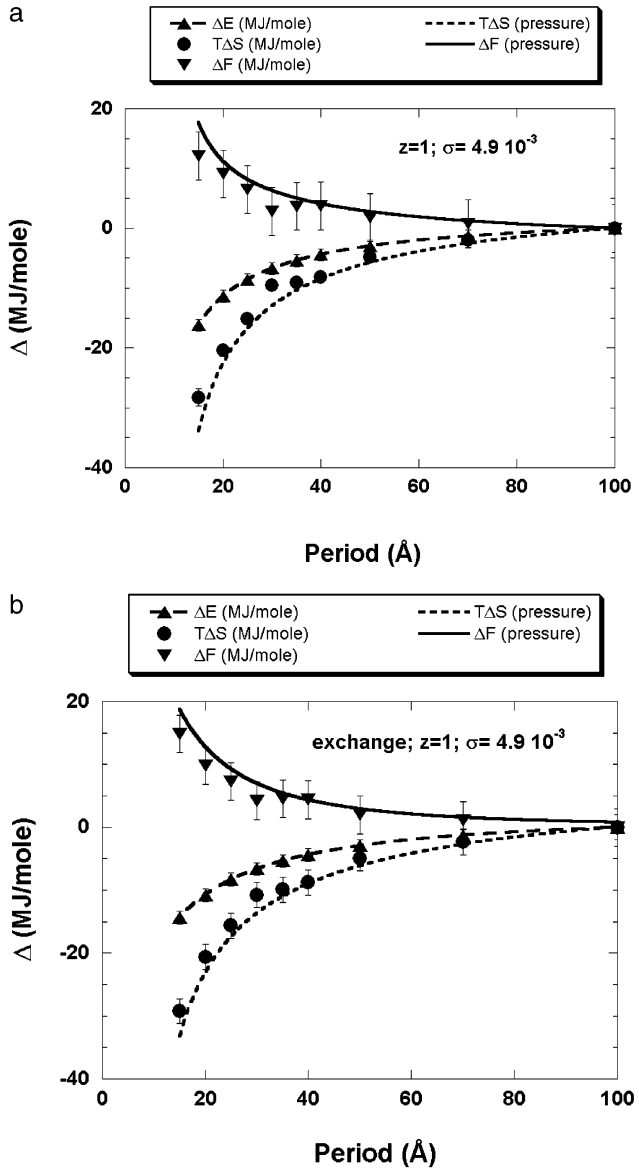

Figure 3. Variation of the interfacial free energy and its energetic and entropic contributions for lamellae neutralized by monovalent counterions without (a) or with (b) ionic exchange between the inner and outer domains.

tion functions of the labile ions. For heterogeneous systems, this derivation leads to the multiparticle correlation expansion:[33]

$$S = S^{(1)} + S^{(2)} + S^{(3)} + ... \quad (5a)$$

$$S^{(1)} = -k\rho_0 \int P(\vec{x}_1) \ln[P(\vec{x}_1)]\, d\vec{x}_1 \quad (5b)$$

$$S^{(2)} = -\frac{k\rho_0^2}{2} \int P(\vec{x}_1)\, d\vec{x}_1 \int P(\vec{x}_2)\, g_2(\vec{x}_1,\vec{x}_2) \ln[g_2(\vec{x}_1,\vec{x}_2)]\, d\vec{x}_2 \quad (5c)$$

$$S^{(3)} = -\frac{k\rho_0^3}{6} \int P(\vec{x}_1)\, d\vec{x}_1 \int P(\vec{x}_2)\, d\vec{x}_2 \int P(\vec{x}_3)\, d\vec{x}_3 \left(g_3(\vec{x}_1,\vec{x}_2,\vec{x}_3) \ln\left[\frac{g_3(\vec{x}_1,\vec{x}_2,\vec{x}_3)}{g_2(\vec{x}_1,\vec{x}_2)\, g_2(\vec{x}_1,\vec{x}_3)\, g_2(\vec{x}_2,\vec{x}_3)}\right] - g_3(\vec{x}_1,\vec{x}_2,\vec{x}_3) + 3g_2(\vec{x}_1,\vec{x}_2)\, g_2(\vec{x}_1,\vec{x}_3) - 3g_2(\vec{x}_1,\vec{x}_2) + 1 \right) \quad (5d)$$

where

$$P(\vec{x}) = \frac{\rho(\vec{x})}{\rho_0}$$

where $\rho(\vec{x})$ is the local ionic density and ρ_0 is the average ionic density.

Equation 5b is the first-order contribution describing the mixing entropy previously introduced in our derivation of the free energy. Equation 5c describes the second-order contribution to the interfacial entropy; it explicitly includes the first contribution from the interionic correlation. The third-order contribution (eq 5d) and further orders are neglected in this calculation. More details on this procedure were already published.[23]

(D) Restricted Grand Canonical Monte Carlo Procedure. Within the classical grand canonical Monte Carlo algorithm,[24,34] the probability of finding a system with N particles in the configuration, $\{\vec{x}_N\}$, is given by

$$P(\{\vec{x}_N\}) = \sum_N \frac{\exp(N\beta\mu)}{N!\Xi}\left(\frac{V}{\Lambda^3}\right)^N \exp(-\beta u(\{\vec{x}_N\})) \quad (6a)$$

with

$$\Xi = \sum_N \frac{\exp(N\beta\mu)}{N!}\left(\frac{V}{\Lambda^3}\right)^N \int_0^1 ... \int_0^1 \exp(-\beta u)\, d\vec{\tau}_1 ... d\vec{\tau}_N \quad (6b)$$

where $\beta = 1/kT$, μ is the chemical potential, and Λ is the de Broglie length. The condition of detailed balance is then used to define the probability of accepting the addition or removal of one particle.[34] In our case, it is not possible to calculate separately the electrostatic energy of each isolated subsystem because they are not electrically neutral, but the energy difference corresponding to the transfer of one cation from a subunit to another is still defined by using Ewald summation, since the *whole system* remains *electrically neutral*. The condition of detailed balance is used again to define the condition of acceptance for such ionic transfer:

$$P(N_1,N_2 \rightarrow N_1+1,N_2-1) = \frac{\exp(\beta\mu)V_1}{(N_1+1)\Lambda^3}\frac{N_2\Lambda^3}{\exp(\beta\mu)V_2}\exp(-\beta\Delta u) = \frac{N_2V_1}{(N_1+1)V_2}\exp(-\beta\Delta u) \quad (7)$$

where V_i is the volume of the subsystem labeled i. As a consequence, knowledge of the ionic chemical potential is not required in this procedure to equilibrate the ionic activity between both subsystems.

During the Monte Carlo procedure, one subunit is selected randomly and one counterion is selected randomly. We proceed then, with an equal probability, either to the displacement of the ion within its subunit by using a classical canonical Monte Carlo procedure or to its removal from the initial subunit and its addition to the second one by using this restricted grand canonical Monte Carlo procedure.

(III) Results and Discussion

(A) Monovalent Counterions. We first evaluate the stability of charged interfaces ($\sigma = 4.9\ 10^{-3}$ e/Å^2) neutralized by sodium counterions (Figure 3a) by using the classical canonical Monte Carlo procedure without ionic exchange between the two subunits. The ionic configurational entropy is a direct measure-

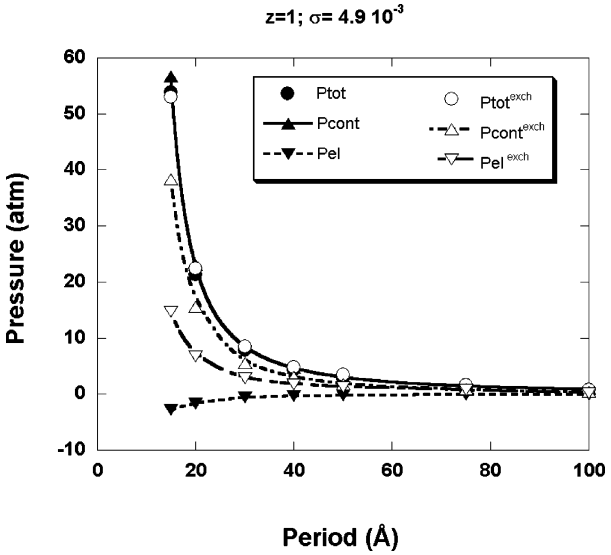

Figure 4. Variation of the interfacial pressure with its contact and electrostatic contributions (see text) calculated for lamellae neutralized by monovalent counterions without (filled symbols) or with (open symbols) ionic exchange between the inner and outer domains.

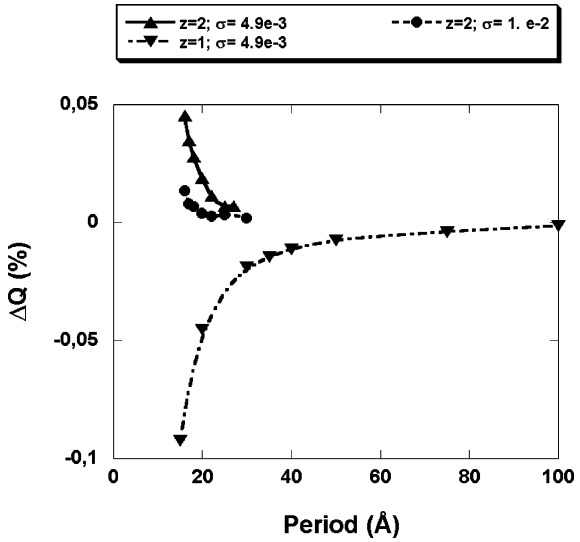

Figure 5. Relative net electric charge of the inner domain resulting from the ionic transfer.

ment of the strong organization of the diffuse layer of confined sodium counterions (see Figure 2). As shown previously,[23] the free energy is strongly repulsive because of the large decrease of the entropy during the compression of the interface despite its electrostatic attraction. Figure 4 also displays the net interfacial pressure and its two contributions: the electrostatic attraction (eqs 3a and b) and the contact repulsion (eq 4). The electrostatic contribution remains negligible, and the swelling pressure results mainly from the difference between the ionic density at contact with the surfaces of the lamellae within the inner and outer domains (see Figure 2). The swelling pressure of such interfaces neutralized by monovalent counterions is thus the consequence of the counterion accumulation within the inner domain. The pressure variation displayed in Figure 4 is fitted by a simple power law which is integrated to determine the free energy variation during the swelling of the lamellae (see Figure 3a), illustrating the validity of our direct derivation of the ionic configurational entropy.

By removing the constraint on the local electroneutrality of each subunit, we expect to relax the strong repulsion resulting from the overlap of the ionic diffuse layer by equating the ionic activity in both domains. The expected reduction of the counterion accumulation in the inner domain (see Figure 2) should strongly decrease the contact pressure exerted by the counterions confined within the dense interlamellar space and thus cancel out the swelling pressure of the interface. As shown in Figure 2, the exchange procedure induces only a small decrease of the ionic density within the dense interlayer and the interfacial free energy (Figure 3b) and its entropic and energetic components remain nearly unchanged, while the net interfacial pressure exhibits no significant decrease of the interlamellar repulsion (Figure 4). As expected from the analysis of the ionic concentration profiles (Figure 2), the contact contribution to the swelling pressure is slightly reduced but the electrostatic contribution becomes significantly repulsive (Figure 4). This behavior results from the repulsion between the net negative charge appearing in the dense interface and the negatively charged lamellae (Figure 5). It is a direct consequence of the reduced transfer of the sodium counterions out of the dense interface [<10% of the total charge of the lamellae (see Figure 5)]. Furthermore, this net negative charge occurring within the dense interlayer strongly restricts the cation removal out of the dense interlayer and inhibits the complete cancellation of the contact pressure exerted by the monovalent counterions at the surface of the lamellae (see Figure 2), while the ionic activities are equilibrated within both domains. By contrast with our expectation, this equilibration has no influence on the net interlayer repulsion because of some compensation between the electrostatic and contact contributions to the swelling pressure.

(B) Divalent Counterions. The interfacial free energy of the same charged interfaces ($\sigma = 4.9\ 10^{-3}$ e/Å^2) neutralized by divalent calcium counterions is nearly independent of the lamellae separation (Figure 6a) because of the perfect matching between its entropic and energetic contributions. An equivalent trend is displayed by the pressure variation (Figure 7) which results from a nearly perfect cancellation between the contact repulsion and the electrostatic attraction. Interionic correlations cancel out the repulsion resulting from the overlap of the diffuse layers surrounding the lamellae, but the interfacial electrostatic coupling,[19]

$$\xi = \left|\frac{z_i e \sigma a_i}{4\pi\epsilon_0\epsilon_r kT}\right| = 0.175$$

where z_i is the counterion valence, is not strong enough to induce a net attraction between the lamellae.

The transfer of the calcium counterions between the inner and outer interfacial domains does not seem to largely modify the interfacial free energy (Figure 6b). Because of the large errors resulting from the direct derivation of the ionic configurational entropy, the more accurate estimate of the free energy variation is given by the integration of the interfacial pressure (Figure 7) which is fitted by a polynomial law. As shown in Figure 6b, the free energy becomes slightly negative at small interlamellar separations because of the reduction of the entropy variation as compared to the energy. This apparently weak attraction is better illustrated by the interfacial pressure (Figure 7) which remains attractive over a large domain of interlamellar separations. This net attraction results from a balance between the enhanced contact repulsion and the strongly attractive interfacial energy (Figure 7). By contrast with charged lamellae neutralized by monovalent counterions, ionic transfer leads now to a large increase (in absolute value) of both the electrostatic attraction and the contact repulsion. This is the consequence of

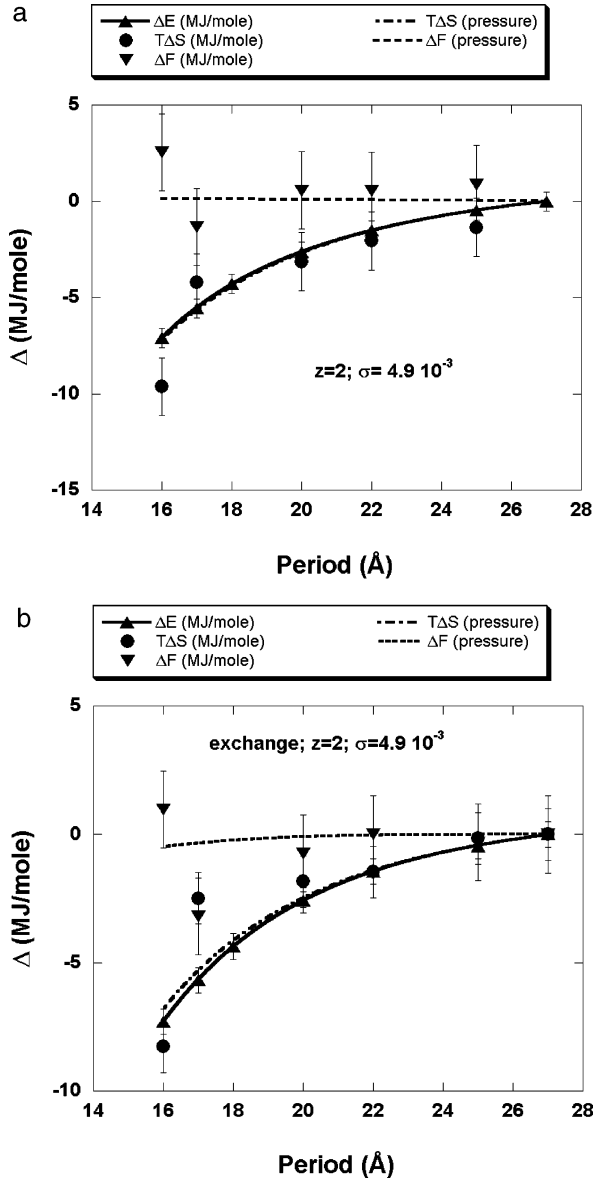

Figure 6. Same as Figure 3 for divalent counterions.

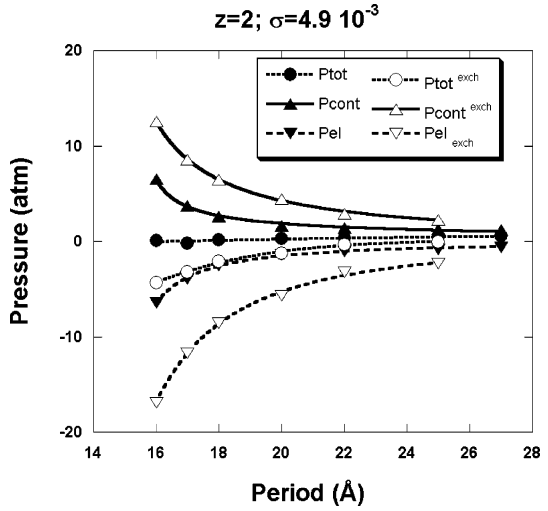

Figure 7. Same as Figure 4 for divalent counterions.

an inversion of the ionic transfer between the two subunits: in contrast with monovalent counterions, the divalent counterions accumulate within the dense interlayer domain (Figure 5).

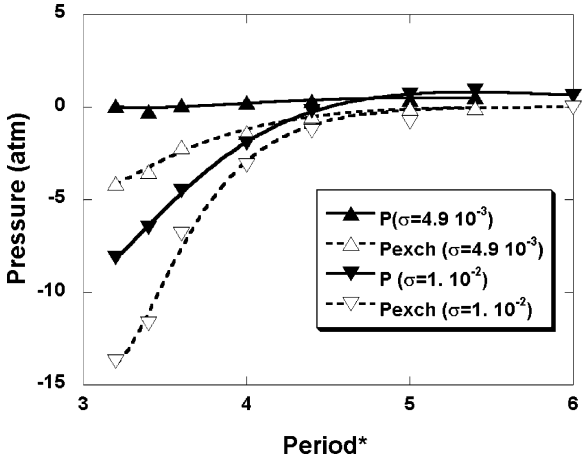

Figure 8. Attracto/repulsive behavior of the charged lamellae neutralized by divalent counterions without (filled symbols) or with (open symbols) ionic exchange. The reduced period, P^*, is defined by the relationship $P^* =$ period/ionic diameter.

To probe the influence of the electrostatic coupling between the charged lamellae, we have increased the surface charge density by a factor of 2. As previously shown, in the absence of ionic transfer,[18,19] the electrostatic attraction increases at small interlamellar separations but disappears at separations of less than two ionic diameters (Figure 8). The finite size of the counterions,[17−19] which is included in the primitive model, is responsible for that repulsive behavior which results also from interionic correlations. It was already shown that this contribution is maximum at an interlamellar separation equal to two ionic diameters.[17−19] After equilibration of the ionic activities between both subunits, we detect a stronger attraction (see Figure 8), while the repulsion previously occurring at larger separations practically disappears. This result may contribute to explain the long range of the attraction measured by AFM between cement [hydrated calciosilicates (CSH)][20] surfaces neutralized by divalent counterions.

As shown in Figure 5, the dense interlayer is still positive, with a net reduction of the relative charge transfer. By integrating the equation of state, it is also possible to determine the variation of the interfacial free energy (Figure 9). In the absence of charge transfer, we detect a small difference between the energy and entropy variation during the swelling of the interface, resulting from the reported attracto/repulsive behavior. By contrast, the ionic transfer induces a significant decrease (in absolute value) of the entropy variation corresponding to the reported attraction.

As a consequence of these numerical simulations, which include interionic correlation effects, the ionic transfer between a dense stack of charged lamellae and a dilute phase is shown to increase the impact of the interionic correlations, enhancing and propagating the net electrostatic attraction previously reported[13−19] between charged lamellae neutralized by divalent counterions. This phenomenon is also shown to modify the apparent ionic exchange capacity of the lamellae by significantly improving the storage capacity of divalent cations at small interlamellar separations. It should be interesting to further investigate this phenomenon for counterions with higher electric charge and in the presence of salt. This breakdown of the local electroneutrality of dense interfaces appears as an extension of the overcharging phenomenon previously reported for charged interfaces in the presence of salt.[35−51] This phenomenon was already shown, in the case of globally neutral interfaces, to enhance the salt absorption capacity of the interlayer and to coincide with an enhancement of the net attraction between

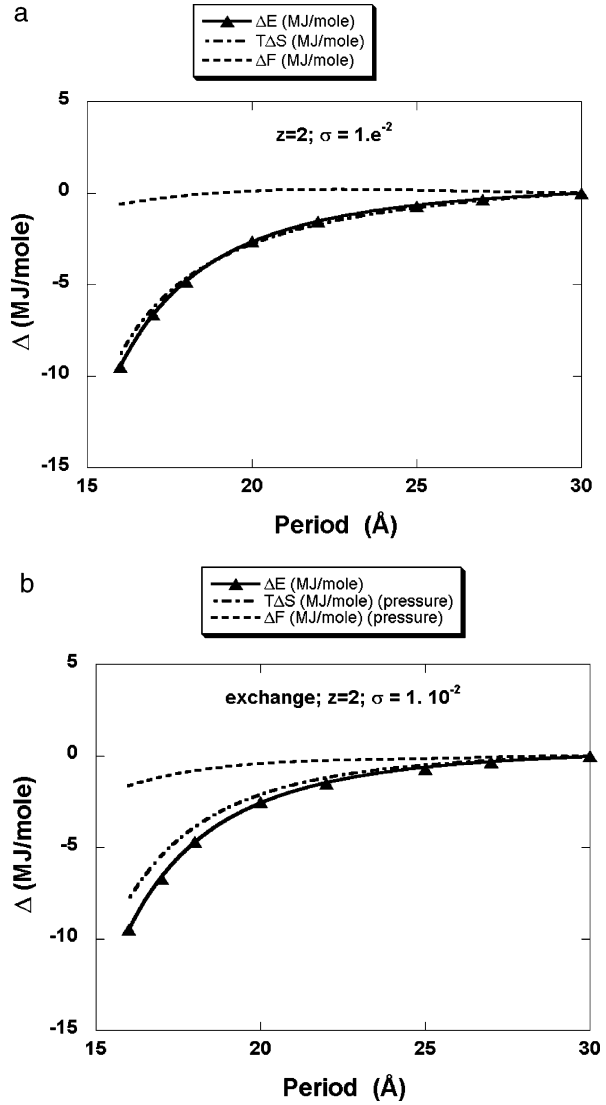

Figure 9. Same as Figure 6 for divalent counterions at the highest electrostatic coupling ($\sigma = 10^{-2}$ e/Å^2).

charged colloids neutralized by di- and trivalent counterions.[35] This transfer of counterions between dense and dilute domains of colloidal suspensions is also expected to occur for other colloidal geometries, including aggregated spheres and cylinders.

Obviously, these results are obtained in the framework of the primitive model[27] which neglects the atomic structure of the charged lamellae and the solvent molecules and is used to investigate only the distribution of charged hard spheres in a dielectric continuum. This approximation is particularly drastic at weak interlamellar separations (less than four solvent diameters), because of the solvent layering[1,52−54] induced by the solid/liquid interface in addition to the local decrease of the solvent permittivity near this interface. For simplicity reasons, these simulations were performed for infinite lamellae. This approximation is justified if the lateral extension of the charged colloids largely exceeds their separation. This requirement is generally fulfilled in suspensions of clay particles which exhibit lateral dimensions up to 1 μm.

(IV) Conclusions

We have performed restricted grand canonical Monte Carlo simulations, in the framework of the primitive model, to test for the influence of the ionic exchange between dense and dilute domains within suspensions of charged lamellae on their mechanical stability. In the presence of monovalent counterions, the transfer of counterions between the dense and dilute subunits has no influence on the swelling pressure despite a significant undercharging of the confined diffuse layers. By contrast, charged lamellae neutralized by divalent counterions exhibit a net enhancement of their attraction induced by the counterion transfer which leads to overcharging of the confined diffuse layer.

Acknowledgment. We cordially thank Drs J. Puibasset and R. Setton for helpful discussions. The Monte Carlo simulations were either performed locally on workstations purchased thanks to grants from Région Centre France or performed at the Gage Computing Facilities (Ecole Polytechnique, France).

References and Notes

(1) Israelachvili, J. C. *Intermolecular and Surface Forces*; Academic Press: London, 1985.
(2) Lyklema, J. *Fundamentals of Interface and Colloid Science*; Academic Press: London, 1991.
(3) Tadros, Th. F. *Solid/Liquid Dispersions*; Academic Press: London, 1987.
(4) Langmuir, I. *J. Chem. Phys.* **1938**, *6*, 873.
(5) Derjaguin, B.; Landau, L. D. *Acta Physicochim. URSS* **1941**, *14*, 635.
(6) Verwey, E. J. W.; Overbeek, J. T. G. *Theory of the Stability of Lyotropic Colloids*; Elsevier: New York, 1948.
(7) Rice, S. A.; Nagasawa, M. *Polyelectrolyte solutions*; Academic Press: New York, 1961.
(8) Marcus, R. A. *J. Chem. Phys.* **1955**, *23*, 1057.
(9) Dubois, M.; Zemb, Th.; Belloni, L.; Delville, A.; Levitz, P.; Setton, R. *J. Chem. Phys.* **1992**, *96*, 2278.
(10) Allahyarov, E.; D'Amico, I.; Löwen, H. *Phys. Rev. Lett.* **1998**, *31*, 8305.
(11) Linse, P.; Lobaskin, V. *J. Chem. Phys.* **2000**, *112*, 3917.
(12) Hribar, B.; Vlachy, V. *J. Phys. Chem. B* **2000**, *104*, 4218.
(13) Van Megen, W.; Snook, I. K. *Mol. Phys.* **1980**, *39*, 1043.
(14) Guldbrand, L.; Jönsson, B.; Wennerstroem, H.; Linse, P. *J. Chem. Phys.* **1984**, *80*, 2221.
(15) Kjellander, R.; Marcelja, S.; Pashley, R. M.; Quirk, J. P. *J. Chem. Phys.* **1990**, *92*, 4399.
(16) Greberg, H.; Kjellander, R.; Akesson, T. *Mol. Phys.* **1997**, *92*, 35.
(17) Valleau, J. P.; Ivkov, R.; Torrie, G. M. *J. Chem. Phys.* **1991**, *95*, 520.
(18) Delville, A.; Pellenq, R. J. M.; Caillol, J. M. *J. Chem. Phys.* **1997**, *106*, 7275.
(19) Pellenq, R. J. M.; Caillol, J. M.; Delville, A. *J. Phys. Chem. B* **1997**, *101*, 8584.
(20) Lesko, S.; Lesniewska, E.; Nonat, A.; Mutin, J. C.; Goudonnet, J. P. *Ultramicroscopy* **2001**, *86*, 11.
(21) Netz, R. R.; Orland, H. *Europhys. Lett.* **1999**, *45*, 726.
(22) Nguyen, T. T.; Rouzina, I.; Shklovskii, B. I. *J. Chem. Phys.* **2000**, *112*, 2562.
(23) Delville, A. *J. Phys. Chem. B* **2004**, *108*, 9984.
(24) Allen, M. P.; Tildesley, D. J. *Computer Simulation of Liquids*; Clarendo Press: Oxford, U.K., 1994.
(25) Legrand, P. *The Surface Properties of Silica*; Wiley & Sons: London, 1998.
(26) Viani, B. E.; Low, Ph. F.; Roth, C. B. *J. Colloid Interface Sci.* **1983**, *96*, 229.
(27) Carley, D. D. *J. Chem. Phys.* **1967**, *46*, 3783.
(28) Cooker, H. *J. Phys. Chem.* **1976**, *80*, 1084.
(29) Heyes, D. M. *Phys. Rev. B* **1994**, *49*, 755.
(30) Hummer, G. *Chem. Phys. Lett.* **1995**, *235*, 297.
(31) Richardson, J. M. *J. Chem. Phys.* **1955**, *23*, 2304.
(32) Nettleton, R. E.; Green, M. S. *J. Chem. Phys.* **1958**, *29*, 1365.
(33) Prestipino, S.; Giaquinta, P. V. *J. Stat. Phys.* **1999**, *96*, 135.
(34) Adams, D. J. *Mol. Phys.* **1974**, *28*, 1241.
(35) Delville, A. *J. Phys. Chem. B* **2002**, *106*, 7860.
(36) Lozada-Cassou, M.; Olivares, W.; Sulbaran, B. *Phys. Rev. E* **1996**, *53*, 522.
(37) Borukhov, I.; Andelman, D.; Orland, H. *J. Phys. Chem. B* **1999**, *103*, 5042.
(38) Deserno, M.; Jimenez-Angeles, F.; Holm, Ch.; Lozada-Cassou, M. *J. Phys. Chem. B* **2001**, *105*, 10983.
(39) Messina, R.; Holm, Ch.; Kremer, K. *Phys. Rev. E* **2001**, *64*, 021405.
(40) Messina, R.; Holm, Ch.; Kremer, K. *Phys. Rev. E* **2002**, *65*, 041805.

(41) Carbajal-Tinoco, M. D.; Gonzales-Mozuelos, P. *J. Chem. Phys.* **2002**, *117*, 2344.
(42) Tanaka, M. *Phys. Rev. E* **2003**, *68*, 061501.
(43) Quesada-Perez, M.; Gonzales-Tovar, E.; Martin-Molina, A.; Lozada-Cassou, M.; Hidalgo-Alvarez, R. *ChemPhysChem* **2003**, *4*, 234.
(44) Tellez, G.; Trizac, E. *Phys. Rev. E* **2003**, *68*, 061401.
(45) Martin-Molina, A.; Quesada-Perez, M.; Galisteo-Gonzalez, F.; Hidalgo-Alvarez, R. *J. Chem. Phys.* **2003**, *188*, 4183.
(46) Wang, K.; Yu Y. X.; Gao, G. H. *Phys. Rev. E* **2004**, *70*, 011912.
(47) Gonzalez-Tovar, E.; Jimenez-Angeles, F.; Messina, R.; Lozada-Cassou, M. *J. Chem. Phys.* **2004**, *120*, 9782.
(48) Patra, Ch. N.; Chang, R.; Yethiraj, A. *J. Phys. Chem. B* **2004**, *108*, 9126.
(49) Forsman, J. *J. Phys. Chem. B* **2004**, *108*, 9236.
(50) Quesada-Perez, M.; Martin-Molina, A.; Hidalgo-Alvarez, R. *J. Chem. Phys.* **2004**, *121*, 8618.
(51) Ravindran, S.; Wu, J. *Langmuir* **2004**, *20*, 7333.
(52) Delville, A. *J. Phys. Chem.* **1993**, *97*, 9703.
(53) Teppen, B. J.; Rasmussen, K.; Bertsch, P. M.; Miller, D. M.; Schäfer, L. *J. Phys. Chem. B* **1997**, *101*, 1579.
(54) Chang, F. R. C.; Skipper, N. T.; Sposito, G. *Langmuir* **1998**, *14*, 1201.